

## **Radical Scavenger-Driven Oxidation Prevention and Structural Stabilization for Efficient and Stable Tin-Based Perovskite Solar Cells**

Seungon Jung<sup>a</sup>, Yunjeong Jang<sup>a</sup>, Hohyun Jung,<sup>a</sup> Yujin Kim<sup>a</sup>, Eunbin Son<sup>b</sup>, Seulgi Jeong,<sup>a</sup> Yihan Zhang,<sup>a</sup> Joohoon Kang<sup>c\*</sup>, Jeong Min Baik<sup>\*de</sup>, Jianfeng Lu<sup>\*f</sup>, and Hyesung Park<sup>\*ag</sup>

<sup>a</sup>KU-KIST Graduate School of Converging Science and Technology, Korea University, 145 Anam-ro, Seongbuk-gu, Seoul 02841, Republic of Korea

<sup>b</sup>Department of Materials Science and Engineering, Ulsan National Institute of Science and Technology, Ulsan 44919, Republic of Korea

<sup>c</sup>Department of Chemical and Biomolecular Engineering, Yonsei University, Seoul 03722, Republic of Korea

<sup>d</sup>School of Advanced Materials Science and Engineering, Sungkyunkwan University (SKKU), Suwon 16419, Republic of Korea

<sup>e</sup>SKKU Institute of Energy Science and Technology (SIEST), Sungkyunkwan University, Suwon 16419, Republic of Korea

<sup>f</sup>State Key Laboratory of Silicate Materials for Architectures, Wuhan University of Technology, Wuhan 430070, China

<sup>g</sup>Department of Integrative Energy Engineering, Korea University, 145 Anam-ro, Seongbuk-gu, Seoul 02841, Republic of Korea

\*Corresponding author

E-mail address: [hyesungpark@korea.ac.kr](mailto:hyesungpark@korea.ac.kr), [jianfeng.lu@whut.edu.cn](mailto:jianfeng.lu@whut.edu.cn), [jbaik97@skku.edu](mailto:jbaik97@skku.edu), [joohoon@yonsei.ac.kr](mailto:joohoon@yonsei.ac.kr)

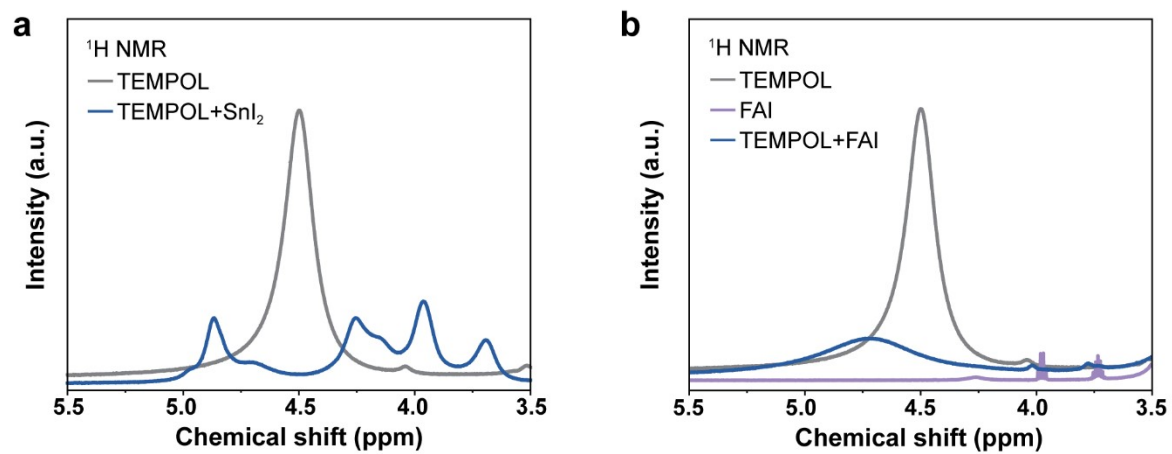


**Fig. S1**  $^1\text{H}$  NMR spectra of (a) TEMPOL and a mixture of TEMPOL with  $\text{SnI}_2$ , and (b) TEMPOL, FAI, and a mixture of TEMPOL with FAI in  $\text{DMSO-d}_6$ .

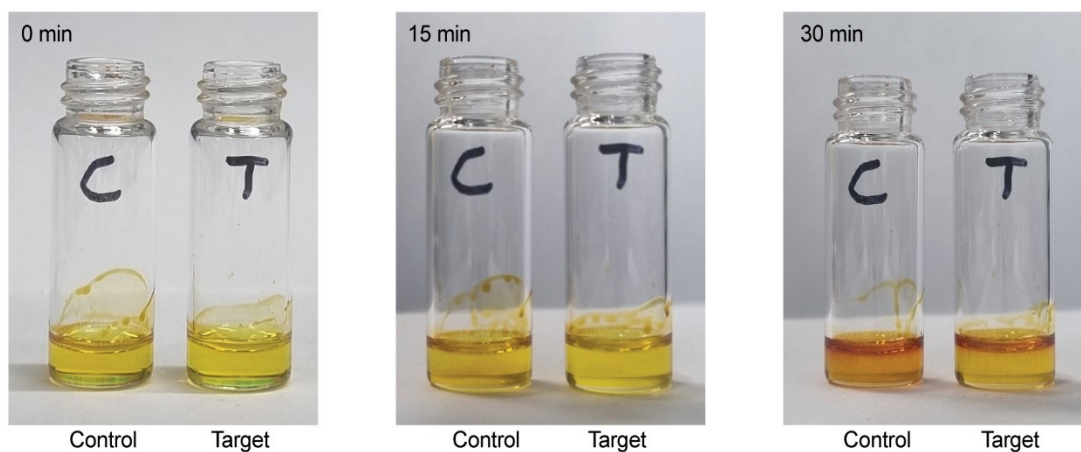


**Fig. S2** Digital photographs of perovskite precursor solutions with and without TEMPOL after exposure to ambient air.

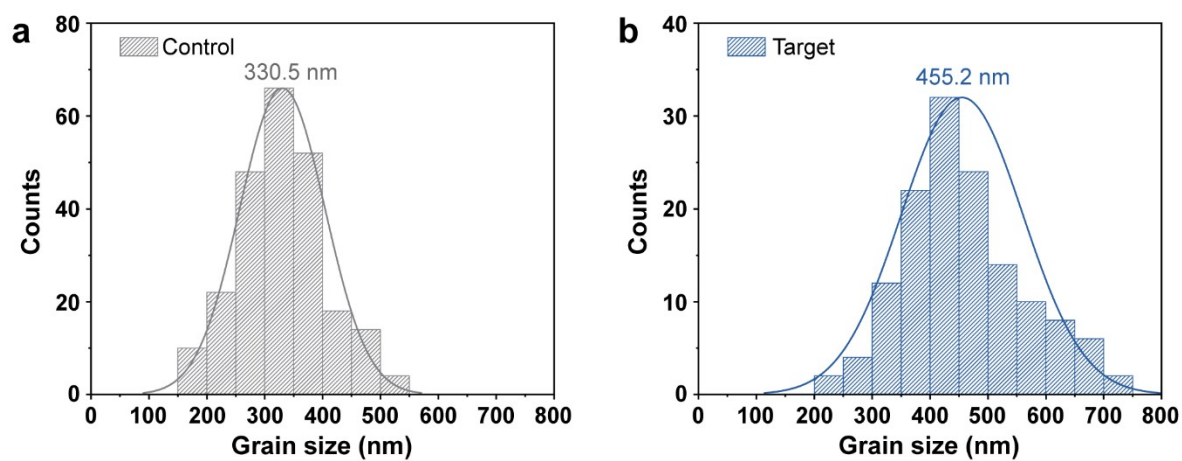


**Fig. S3** Grain size distribution extracted from SEM images of (a) control and (b) target films.

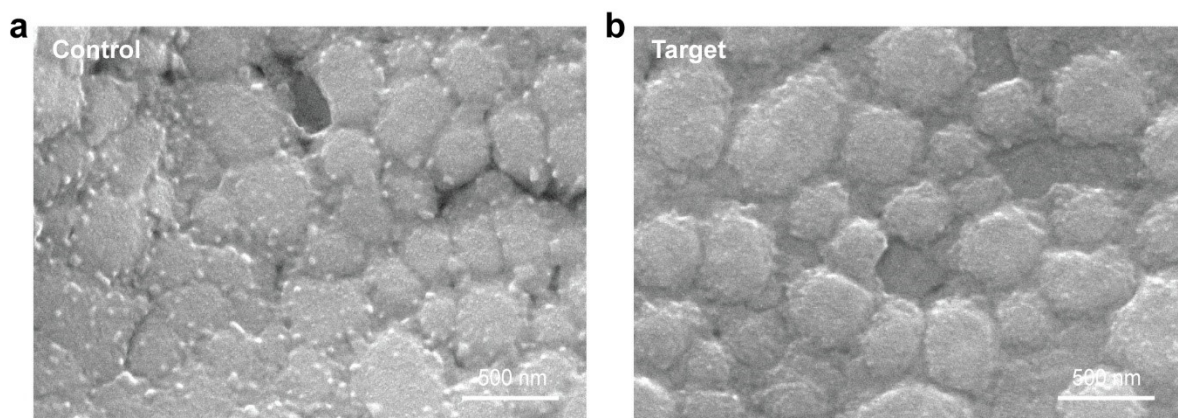


**Fig. S4** SEM images of the buried interface between the PEDOT:PSS and perovskite layers in the (a) control and (b) target films.

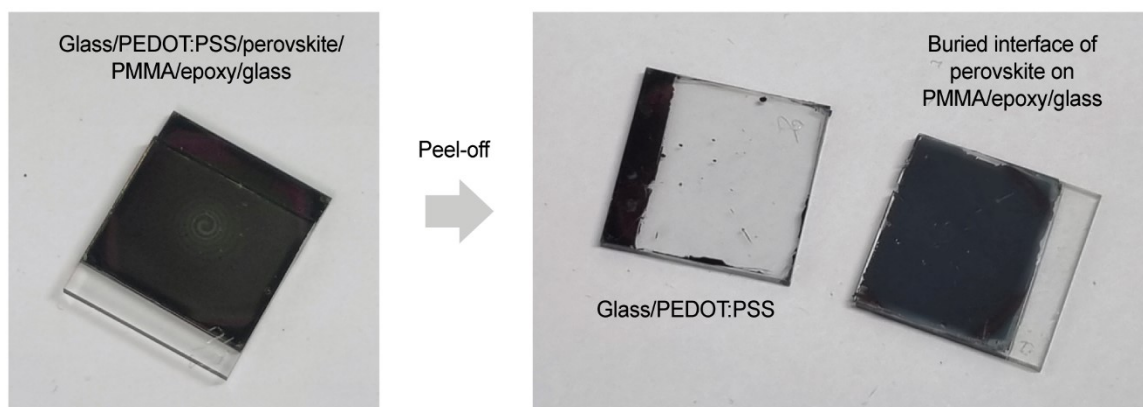


**Fig. S5** Photographs illustrating the mechanical peeling process used to expose the buried interface between the PEDOT:PSS and perovskite layers. To prepare samples, a glass/PEDOT:PSS/perovskite stack was first coated with a protective polymer layer. A 1:1 vol% solution of PMMA (950 PMMA A6, Kayaku Advanced Materials) in CB was spin-coated onto the perovskite surface at 2,000 rpm for 30 s, followed by thermal annealing at 80 °C for 5 min. A small drop of UV-curable epoxy resin (E132, Ossila) was then applied on top of the PMMA layer, and a secondary glass slide was gently placed on top. The assembly was exposed to UV light for 5 min to cure the epoxy and secure the top glass. Mechanical separation was subsequently performed by gently peeling apart the two glass substrates, enabling delamination of the perovskite layer near the PEDOT:PSS interface.

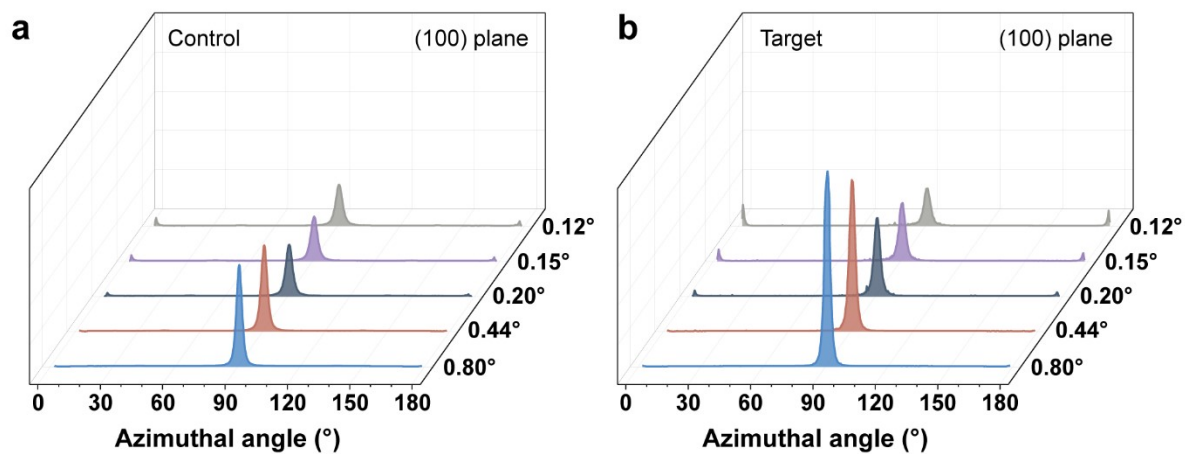


**Fig. S6** Azimuthal intensity profiles for the (100) plane along the scattering ring at around  $q_r = 1.0 \text{ \AA}^{-1}$  for (a) control and (b) target films.

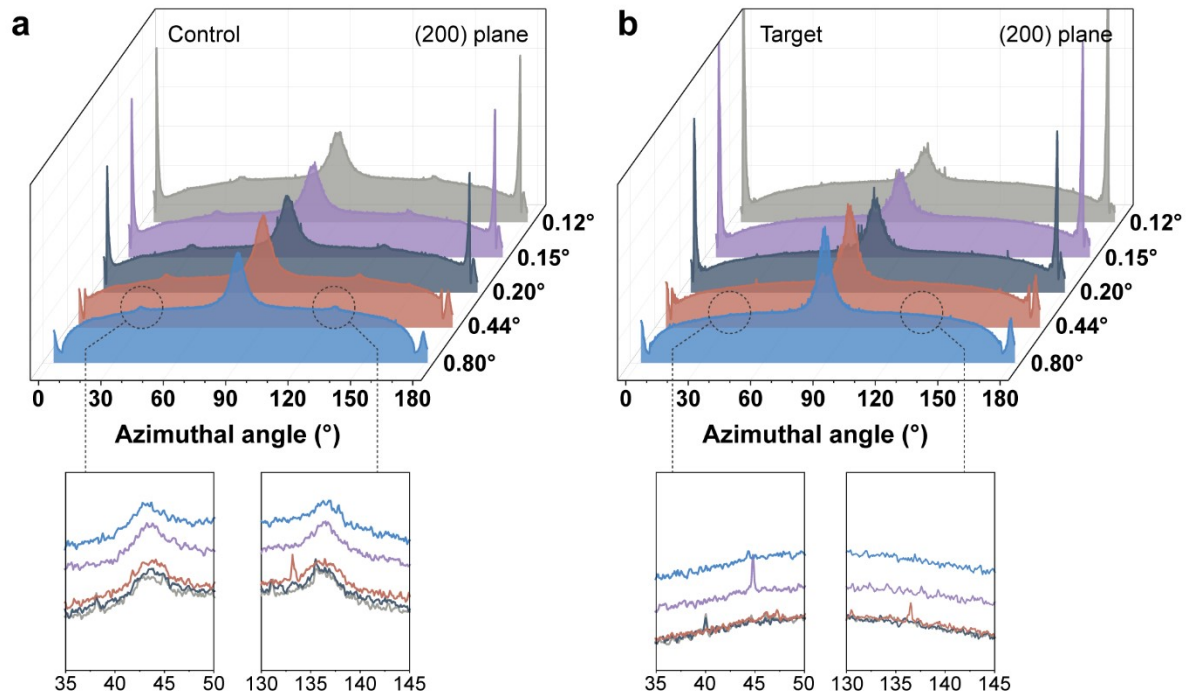


**Fig. S7** Azimuthal intensity profiles for the (200) plane along the scattering ring at around  $q_r = 2.0 \text{ \AA}^{-1}$  for (a) control and (b) target films, with a zoom-in view at  $\chi = 35^\circ$  to  $50^\circ$  and  $130^\circ$  to  $145^\circ$ .



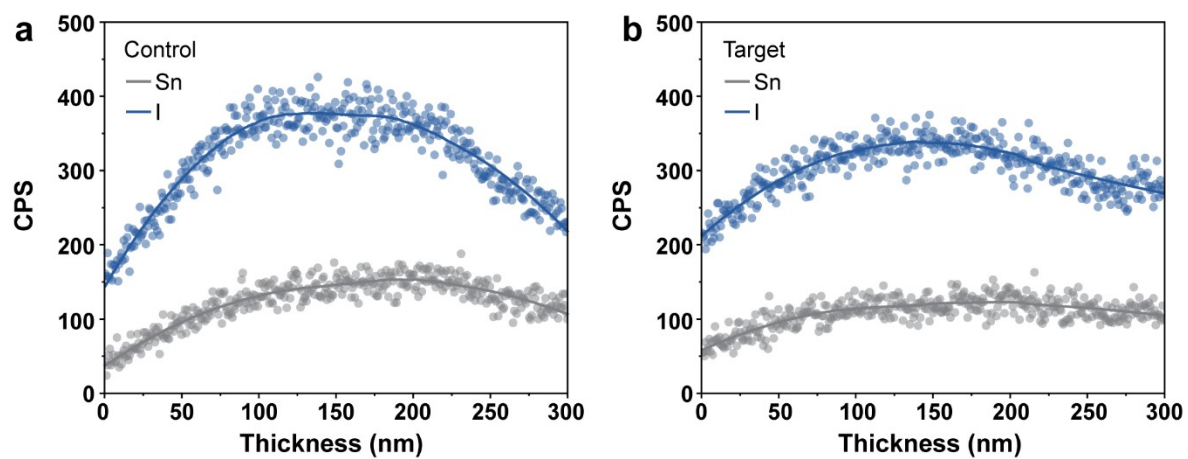


**Fig. S8** Cross-sectional SEM-EDS line scan profiles of the Sn/I atomic ratio for (a) control and (b) target films.

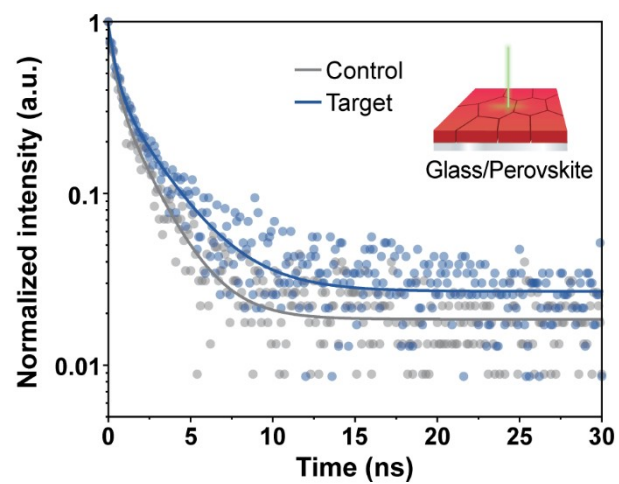


**Fig. S9** TRPL spectra of control and target films.

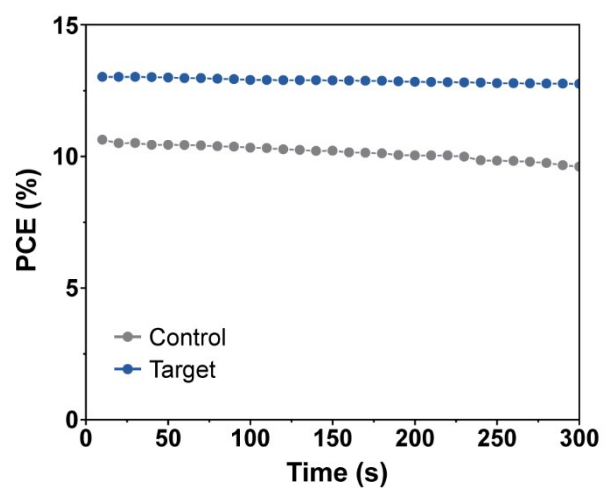


**Fig. S10** Steady-state power output of the PSCs under continuous 1-sun illumination.

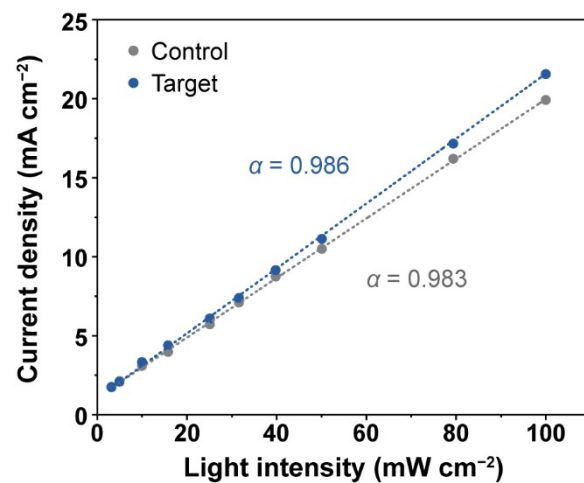


**Fig. S11** Light-intensity dependence of  $J_{sc}$  in the PSCs.

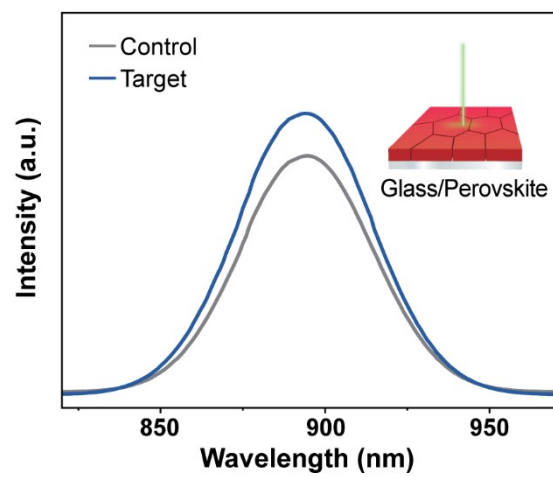


**Fig. S12** PL spectra of control and target films.

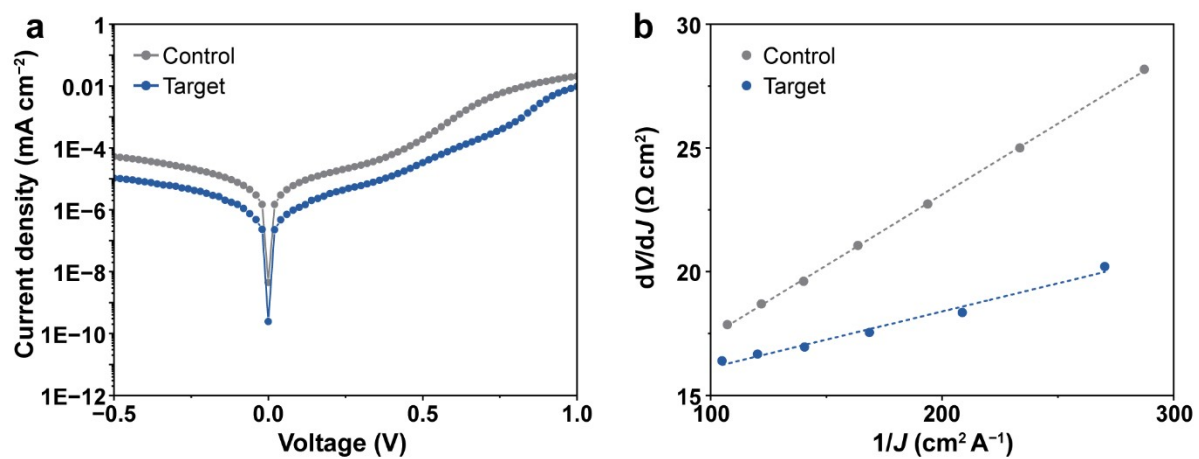


**Fig. S13** (a) Dark current characteristics of the PSCs. (b)  $dV/dJ$  versus  $1/J$  plots derived from dark current measurements.

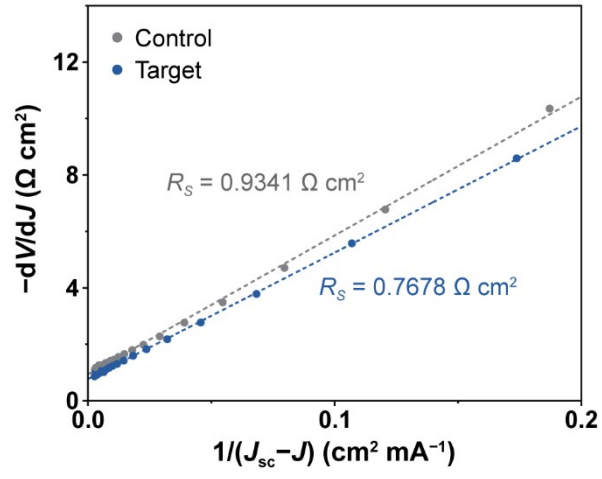


**Fig. S14**  $-dV/dJ$  versus  $1/(J_{sc}-J)$  plots derived from  $J$ - $V$  measurements.

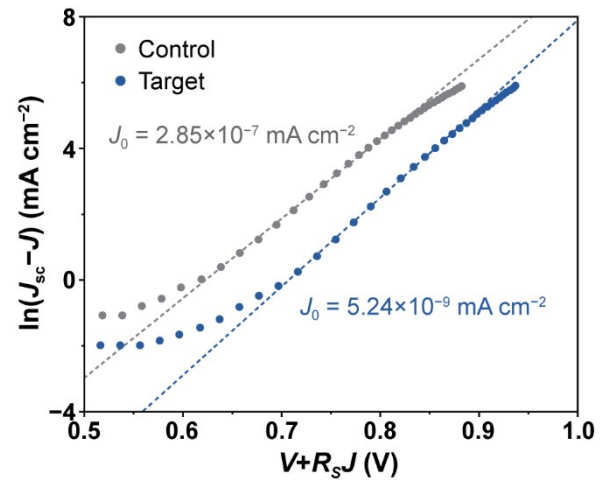


**Fig. S15**  $\ln(J_{sc}-J)$  versus  $V+R_sJ$  plots derived from  $J-V$  measurements.



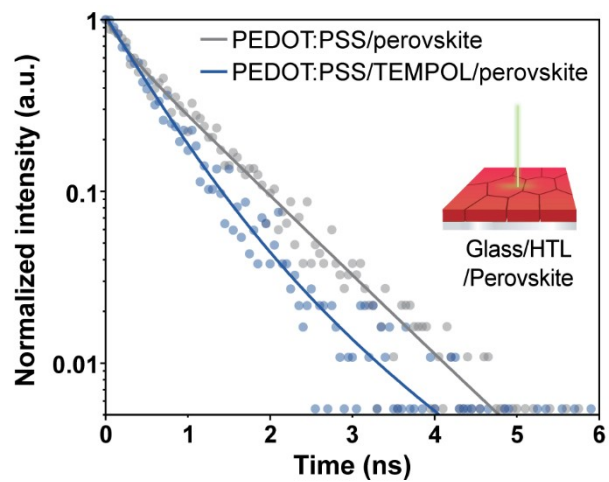


**Fig. S16** TRPL spectra of perovskite films on PEDOT:PSS with and without the TEMPOL interlayer.

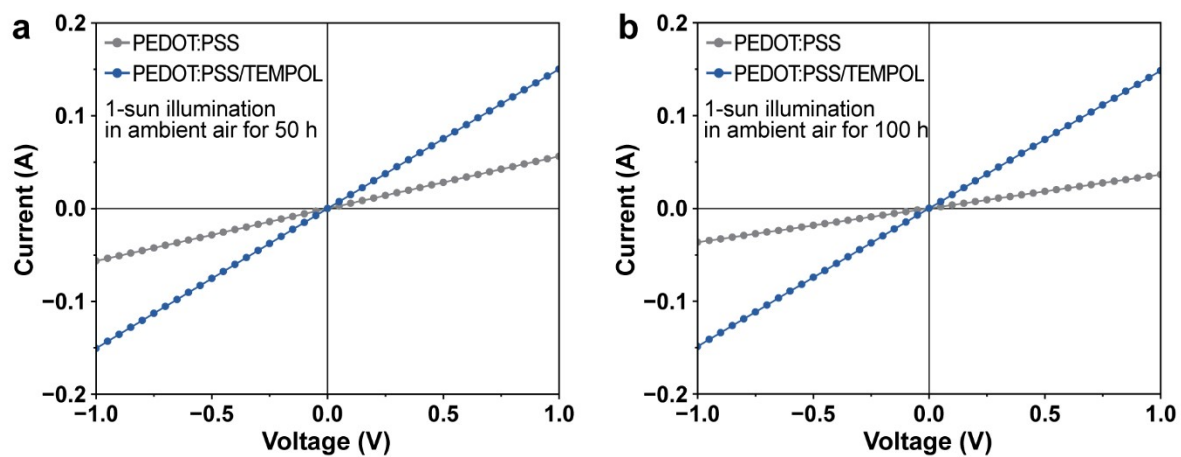


**Fig. S17** Electrical conductivity of PEDOT:PSS and PEDOT:PSS/TEMPOL films after aging for (a) 50 h and (b) 100 h under 1-sun illumination in ambient air.